



This is a repository copy of *Higher Order Frequency Response Functions in Nonlinear System Identification*.

White Rose Research Online URL for this paper:
<http://eprints.whiterose.ac.uk/78657/>

Monograph:

Tomlinson, G.R. and Billings, S.A. (1991) Higher Order Frequency Response Functions in Nonlinear System Identification. Research Report. Acse Report 432 . Dept of Automatic Control and System Engineering. University of Sheffield

Reuse

Unless indicated otherwise, fulltext items are protected by copyright with all rights reserved. The copyright exception in section 29 of the Copyright, Designs and Patents Act 1988 allows the making of a single copy solely for the purpose of non-commercial research or private study within the limits of fair dealing. The publisher or other rights-holder may allow further reproduction and re-use of this version - refer to the White Rose Research Online record for this item. Where records identify the publisher as the copyright holder, users can verify any specific terms of use on the publisher's website.

Takedown

If you consider content in White Rose Research Online to be in breach of UK law, please notify us by emailing eprints@whiterose.ac.uk including the URL of the record and the reason for the withdrawal request.



eprints@whiterose.ac.uk
<https://eprints.whiterose.ac.uk/>

~~RAMBOX~~

Higher Order Frequency Response Functions in Nonlinear System Identification

G R Tomlinson
Department of Engineering
University of Manchester
Manchester
UK

S A Billings
Department of Automatic Control and Systems Engineering
University of Sheffield
Sheffield
UK

Research Report No 432

June 1991

HIGHER ORDER FREQUENCY RESPONSE FUNCTIONS IN NONLINEAR SYSTEM IDENTIFICATION

G.R. Tomlinson, Professor, Department of Engineering, University of Manchester, Manchester, UK.
S.A. Billings, Professor, Department of Automatic Control and Systems Engineering, University of Sheffield, Sheffield, UK.

ABSTRACT

This paper describes higher order frequency response functions (FRF's) and their role in the identification of nonlinear systems. Higher order FRF's only exist for nonlinear systems and have the property that they visually demonstrate how energy is transferred from one frequency to another, a unique characteristic of nonlinear structures and systems. The determination of these FRF's can be approached from two principal directions; using sine excitation by directly measuring the higher order transfer functions which approximate to higher order FRF's or using nonlinear time series methods and probing these to extract the FRF's. In this paper, these approaches are described in relation to simple nonlinear problems and their role in future system methodologies discussed. It is shown that if reliable higher order spectra can be obtained they offer a positive and useful means of practically diagnosing a class of nonlinear structural dynamics problems.

1. INTRODUCTION

The use of the classical one dimensional frequency response function in system identification is a very common occurrence, particularly in the domain of experimental modal analysis. The use of higher order frequency response functions in system identification is still very embryonic. The major use of higher order spectra is in the field of fluid-structure interaction where there are several examples of energy transfer mechanisms, in some cases identified via the bi-spectrum (or second order frequency response function, which have been shown to account for low frequency, large oscillatory motion of Tension Leg Platforms induced by a quadratic nonlinear mechanism) which have allowed more accurate predictions of the wave forces on offshore structures.¹ However, the use of higher order frequency response functions in structural dynamics, particularly of aerospace and aircraft structures, has been very limited. The principal reasons for this are likely to be due to :

- (a) the fact that they only exist if a structure displays nonlinearity and the identification/interpretation of structural nonlinearity in a practical environment is still a difficult area and,
- (b) there are a few straightforward methods of measuring higher order frequency response functions; they are still a new science and their usefulness still has to be fully established.

This paper describes two procedures for determining higher order frequency response functions which could form the basis of an approach to predicting the behaviour of nonlinear structures.

The paper begins by showing how higher order frequency response functions offer an insight into structural nonlinearity and then moves on to two approaches for obtaining them, one which utilises sinusoidal excitation to directly extract the higher order transfer functions and the other which fits nonlinear difference models to time data which is then probed to extract the higher order frequency response functions.

2. TRANSFER FUNCTIONS AND FREQUENCY RESPONSE FUNCTIONS

In the system identification of linear structures the terminology transfer or frequency response function implies the same thing; the relationship between the input(s) and the output(s) in the frequency domain. These functions satisfy the principle of superposition and are invariant with respect to the type of input.

However, in order to apply these concepts to nonlinear structures we need to be more specific. In fact, even with linear structures there is a difference between what we actually measure and what we calculate due to the fact that we always deal in practise with a truncated model. Thus we need to define transfer functions and frequency response functions.

In this paper we define transfer functions for either linear or nonlinear structures as the measured relationships between the input(s) and the output(s). Frequency response functions are input/output relationships which are calculated from either simulation, analytical or other derived procedures.

For example, if we consider the equation governing the well known Duffing oscillator (a good benchmark model for nonlinear structures) we can write down equations governing the higher order transfer functions as below. The Duffing oscillator with viscous damping is,

$$m\ddot{y}(t) + c\dot{y}(t) + ky(t) + k_3y(t)^3 = x(t) \quad (1)$$

If $x(t)$ is considered to be a sinusoidal input waveform, the Fourier transforms (of the input and output signals) can be computed at the excitation frequency ' ω ' to give the first

200165450



order and the higher order transfer functions (TF's) i.e.

$$\begin{aligned} \text{TF}_1(j\omega) &= \frac{Y(j\omega)}{X(j\omega)} \\ \text{TF}_3(j\omega) &= \frac{4Y(j3\omega)}{X(j\omega)^3} \\ \text{TF}_n(j\omega) &= \frac{2^{n-1}Y(jn\omega)}{X(j\omega)^n}; n=1, 3, 5 \end{aligned} \quad (2)$$

$Y(j\omega)$ is the fundamental output term at the input frequency ω and $Y(j3\omega)$ etc. are the displacement responses at the third, fifth etc. higher harmonics. The coefficient 2^{n-1} arises from the symmetry property. Note that all the even TF's are zero.

The transfer functions are complex and thus the TF's convey both gain and phase information. The higher order TF's convey the fact that energy is transferred for a nonlinear structure.

Obviously, if one were involved in a ground vibration test (GVT) of an aircraft then the quantities shown in equation (2) could be obtained if sine excitation were used.

What do these TF's look like? Figure 1(a), (b) shows the first and third order TF's respectively using numerical simulation for the model given in equation (1) with the parameters $m = 1$, $c = 10$, $k_1 = 10^4$, $k_3 = 10^{10}$. Two levels of excitation were used, a low level below which the TF's were invariant (i.e. the TF's were homogeneous) and therefore could be classed as linear, and a high level where the 'jump' phenomenon is observed close to the fundamental natural frequency of $\omega_n = 100$ rad/s.

There are three important results present in Figures 1(a), (b). The first is that the third order TF exists and exhibits a resonance at $\omega_n/3$ i.e. 33 rad/s together with a resonance at the sine frequency as the first order TF. The second result is that significant distortion (namely a bifurcation) exists in both the first and third order TF's at the fundamental resonance at the higher excitation level. Thirdly, it is possible to identify a third order TF at a low excitation level even when the first order TF "appears" to be linear.

The absence of any second order TF's is due to the absence of a quadratic term in the simulated equation of motion. However, if equation (1) was modified such that the cubic term was replaced by a quadratic term then both odd and even harmonics exist and the higher order TF's are as shown in Figures 2(a), (b). These exhibit, as expected, resonances at $\omega_n/3$, $\omega_n/2$ and ω_n . Thus we have a procedure which could fit into a conventional stepped sine modal test and form the basis of a nonlinear diagnostic procedure that should provide information on the modes which exhibit nonlinearity. Having established that in principle, higher order transfer functions can be measured the next question we ask is how do these measured transfer functions relate to frequency response functions.

Frequency response functions for the class of nonlinearities which can be represented as continuous (e.g. polynomials in displacement and/or velocity) can be effectively represented using the Volterra series with the harmonic input³

$$x(t) = X_1 e^{j\omega_1 t} \quad (3)$$

The output response is then,

$$\begin{aligned} y(t) &= X_1 e^{j\omega_1 t} \int_{-\infty}^{\infty} h_1(\tau_1) e^{-j\omega_1 \tau_1} d\tau_1 \\ &+ X_1^2 e^{j2\omega_1 t} \int_{-\infty}^{\infty} \int_{-\infty}^{\infty} h_2(\tau_1, \tau_2) e^{-j(\omega_1 \tau_1 + \omega_1 \tau_2)} d\tau_1 d\tau_2 \\ &+ \dots X_1^n e^{jn\omega_1 t} \int_{-\infty}^{\infty} \dots \int_{-\infty}^{\infty} h_n(\tau_1, \dots, \tau_n) e^{-j(\omega_1 \tau_1 + \dots + \omega_1 \tau_n)} d\tau_1 \dots d\tau_n \end{aligned} \quad (4)$$

Recognising that the terms inside the integrals represent respectively the one dimensional Fourier transform, the two dimensional Fourier transform up to the n th dimensional transform, equation (4) can be written as,

$$\begin{aligned} y(t) &= H_1(j\omega) X_1 e^{j\omega_1 t} + H_2(j\omega_1, j\omega_1) X_1^2 e^{j2\omega_1 t} \\ &+ \dots H_n(j\omega_1, \dots, j\omega_1) X_1^n e^{jn\omega_1 t} \end{aligned} \quad (5)$$

If we assume a harmonic input we can again define the higher order FRF's in a similar way to the transfer functions i.e.

$$H_n(j\omega, \dots, j\omega) = \frac{2^{n-1} Y(jn\omega)}{X(j\omega)^n} \quad (6)$$

In order to establish the difference between the TF's and the FRF's we need to examine the difference between a harmonic input $x(t) = X e^{j\omega t}$ and a sinusoidal input $x(t) = X \cos \omega t$.

Noting that $X e^{\pm j\omega t} = X(\cos \omega t \pm j \sin \omega t)$, then

$$\begin{aligned} X \cos \omega t &= \frac{X}{2} (e^{j\omega t} + e^{-j\omega t}) \\ y(t) &= \frac{X}{2} [H_1(j\omega) e^{j\omega t} + H_1(-j\omega) e^{-j\omega t}] \\ &+ \left(\frac{X}{2}\right)^2 [H_2(j\omega, j\omega) e^{j2\omega t} + H_2(-j\omega, -j\omega) e^{-j2\omega t} \\ &+ H_2(j\omega, -j\omega) e^{j\omega t} + H_2(-j\omega, j\omega) e^{-j\omega t}] \\ &+ \left[\frac{X}{2}\right]^3 [H_3(j\omega, j\omega, j\omega) e^{j3\omega t} + H_3(-j\omega, -j\omega, -j\omega) e^{-j3\omega t} \\ &+ H_3(j\omega, j\omega, -j\omega) e^{j\omega t} + H_3(j\omega, -j\omega, -j\omega) e^{-j\omega t} \\ &+ H_3(j\omega, -j\omega, j\omega) e^{j\omega t} + H_3(-j\omega, j\omega, -j\omega) e^{-j\omega t} \\ &+ H_3(-j\omega, -j\omega, j\omega) e^{-j\omega t} + H_3(-j\omega, j\omega, j\omega) e^{j\omega t}] \end{aligned} \quad (7)$$

Defining the first order transfer functions as before,

$$TF_1(j\omega) = \frac{Y(j\omega)}{X(j\omega)} \quad (8)$$

Using equation (7), and noting the symmetry properties i.e. $H_3(j\omega, j\omega, -j\omega) = H_3(j\omega, j\omega, j\omega)$ etc,

$$TF_1(j\omega) = H_1(j\omega) + 6H_3(j\omega, j\omega, -j\omega)\frac{X_1^2}{8} + \dots + H_n(j\omega, j\omega, \dots, -j\omega)n\left[\frac{X_1}{2}\right]^{n-1}; n=1,3,5.. \quad (9)$$

We see that only the odd order FRF's contribute to the response and that it is these terms which interact with the first order FRF $H_1(j\omega)$ to cause the distortion. The level of the distortion in $H_1(j\omega)$ is directly related to the amplitude of the excitation i.e. the coefficients in front of the $H_n(j\omega)$ terms. Thus any nonlinear structure governed by the above equations (i.e. polynomial type nonlinearity) will always display distortion in the first order FRF if excited by a sine wave, the significance of the distortion being dependent upon the level of the excitation.

3. HIGHER ORDER FRF'S FROM NARMAX MODELS

The NARMAX⁴ (Nonlinear AutoRegressive Moving Average model for exogenous inputs) model for a single input/single output system is a difference equation of the form,

$$y(t) = dc + F^{\ell}[y(t-1), \dots, y(t-n_y), u(t-d), \dots, u(t-n_u), e(t-1), \dots, e(t-n_e)] + e(t) \quad (10)$$

where $y(t)$, $u(t)$, $e(t)$ are the sampled output, input and prediction error sequences respectively. d is the system time delay, ℓ the degree of nonlinearity and 'dc' a constant term. In this paper F^{ℓ} will be taken as a polynomial although equation (9) is not restricted to this case. This approach begins in the time domain where the objective is to fit an optimum number of terms on the RHS of equation (9) whose contributions to the output are significant. The methods used for detecting the structure i.e. which terms are significant, parameter estimation and model validation can be found in the papers by Billings et al^{5,6}. A simple example of how the procedure works is described below.

Consider a nonlinear differential equation given by,

$$m\ddot{y} + c\dot{y} + k_1y + k_3y^3 = u \quad (11)$$

Using a simple Euler approximation,

$$y = \frac{y(t+1) - 2y(t) + y(t-1)}{T^2}$$

$$\dot{y} = \frac{y(t) - y(t-1)}{T}; \quad t = \text{sample instant}$$

$$T = \text{sample period.}$$

We can discretise equation (11) to give,

$$\frac{m}{T^2} [y(t+1) - 2y(t) + y(t-1)] + \frac{c}{T} [y(t) - y(t-1)]$$

$$+ k_1y(t) + k_3y(t)^3 = u(t)$$

$$\text{i.e. } y(t) + \left[\frac{TC}{m} - 2 + \frac{T^2k_1}{m} \right] y(t-1)$$

$$+ \left[1 - \frac{TC}{m} \right] y(t-2)$$

$$+ \frac{k_3T^2}{m} y(t-1)^3 = \frac{T^2}{m} u(t-1) \quad (12)$$

$$\text{i.e. } y(t) = a_1y(t-1) + a_2y(t-2) + a_3y(t-1)^3 + a_4u(t-1)$$

Using N sampled data points we get,

$$\begin{bmatrix} y_2 \\ y_3 \\ \vdots \\ y_N \end{bmatrix} = \begin{bmatrix} y_1 & y_0 & u_1 & y_1^3 \\ \vdots & \vdots & \vdots & \vdots \\ y_{N-1} & y_{N-2} & u_{N-1} & y_{N-1}^3 \end{bmatrix} \begin{bmatrix} a_1 \\ a_2 \\ a_3 \\ a_4 \end{bmatrix}$$

$$\{y\} = [\varphi]\{\beta\} \quad (13)$$

$$\hat{\beta} = \left[[\varphi]^T[\varphi] \right]^{-1} [\varphi]^T\{y\} \quad (14)$$

$$\hat{\beta} = \text{least squares estimate of } \{\beta\} \quad (14)$$

If we include additive noise on the output we have,

$$z(t) = y(t) + e(t) \quad (15)$$

then,

$$z(t) = a_1z(t-1) + a_2z(t-2) + a_3z(t-1)^3 + a_4u(t-1) + \{e(t) - a_1e(t-1) - 3a_3e(t-1)^2 - 3a_3z(t-1)e(t-1)^2 - 3a_3z(t-1)^2e(t-1)\} \quad (16)$$

Thus we see that we introduce multiplicative noise terms due to the nonlinearity which require inclusion of a noise model:

$$\{y\} = [\varphi]\{\beta\} + \{e\} \quad (17)$$

The number of terms introduced is thus dependent on the order of the nonlinearity and to a first approximation there would be:

$$(n_y + n_u + n_e)^{\ell}/\ell! \quad (18)$$

where n_y , n_u and n_e represent the number of terms in the output, input and the noise model and ' ℓ ' is the degree of the nonlinearity.

Thus for the equation shown (i.e. the Duffing oscillator) we

could have,

$$(3 + 1 + 5)^3/3! = 121 \text{ terms} \quad (19)$$

This means that in equation (13) $[\varphi]^T[\varphi] = 121^2$. In order to optimise the solution to this problem an orthogonal estimator algorithm was developed by Billings et al which rapidly identifies the significant terms⁶. A typical output of this estimator is shown in Table 1 with the model predicted response overlaid on the actual response. To extract the higher order FRF's, one simply discards the noise model and uses the method of Harmonic Probing⁷. This method is based on the procedure described earlier whereby the input is assumed to be of the form $u(t) = e^{j\omega t}$. If we use an example, it is easy to see just how one obtains the higher order FRF's. If we obtain a NARMAX model of the form,

$$y(t) = ay(t-1) + cy(t-1)^2 + bu(t-1) \quad (20)$$

and let $u(t-1) = e^{j\omega(t-1)}$

$$\therefore y(t-1) = H_1(\omega)e^{j\omega(t-1)}$$

$$\begin{aligned} \therefore H_1(\omega)e^{j\omega t} &= aH_1(\omega)e^{j\omega(t-1)} + be^{j\omega(t-1)} \\ &+ c[H_1(\omega)e^{j\omega(t-1)}]^2 \end{aligned} \quad (21)$$

Equating coefficients of $e^{j\omega t}$ gives,

$$H_1(\omega) = \frac{be^{-j\omega}}{1 - ae^{-j\omega}} \quad (22)$$

Similarly to calculate the second order FRF $H_2(\omega_1, \omega_2)$ simply let

$$u(t) = e^{j\omega_1 t} + e^{j\omega_2 t}$$

$$u(t-1) = e^{j\omega_1(t-1)} + e^{j\omega_2(t-1)}$$

$$y(t) = H_1(\omega_1)e^{j\omega_1 t} + H_1(\omega_2)e^{j\omega_2 t}$$

$$+ 2H_2(\omega_1, \omega_2)e^{j(\omega_1 + \omega_2)t}$$

$$+ H_2(\omega_1, \omega_1)e^{j2\omega_1 t}$$

$$+ H_2(\omega_2, \omega_2)e^{j2\omega_2 t}$$

$$y(t-1) = H_1(\omega_1)e^{j\omega_1(t-1)} + H_1(\omega_2)e^{j\omega_2(t-1)} \text{ etc.} \quad (23)$$

equating coefficients of $e^{j(\omega_1 + \omega_2)t}$ gives,

$$H_2(\omega_1, \omega_2) = \frac{cH_1(\omega_1)H_1(\omega_2)e^{j(\omega_1 + \omega_2)}}{1 - ae^{-j(\omega_1 + \omega_2)}} \quad (24)$$

The process can be repeated for $H_3(\omega_1, \omega_2, \omega_3)$ to the H_n 's. Figures 3 and 4 show respectively the leading diagonals and the full 3D plots from harmonically probing the NARMAX models of the equations,

$$\begin{aligned} y + 10\dot{y} + 10^4 y + 10^{10} y^3 &= e^{j\omega t} \\ y + 10\dot{y} + 10^4 y + 10^7 y^2 &= e^{j\omega t} \end{aligned} \quad (25)$$

4. INTERPRETATION OF THE HIGHER ORDER FRF'S

The interpretation of the higher order FRF's is not straightforward. Indeed, once one goes above the third order FRF one would need 'four dimensional space'. In fact, simplifications can be made whereby at the level of H_3 and above, use is made of three dimensional plots under the conditions that, for $H_3(\omega_1, \omega_2, \omega_3)$ for example, $\omega_3 = \omega_1$; ω_2 and $\omega_1 \neq \omega_2$ and one would obtain several plots which have the same format as the H_2 's.

If we taken an example of an $H_2(\omega_1, \omega_2)$ function we can demonstrate the important properties. The equation,

$$\ddot{y}(t) + 10\dot{y}(t) + 10^4 y(t) + 10^7 y(t)^2 = 0.6 \cos \omega t \quad (26)$$

which was used earlier can be harmonically probed to give,

$$H_1(j\omega) = \frac{1}{10^4 - \omega^2 + j10\omega} \quad (27)$$

$$H_2(j\omega_1, j\omega_2) = -10^7 H_1(j\omega_1)H_1(j\omega_2)H_1(j\omega_1 + j\omega_2) \quad (28)$$

where,

$$H_1(j\omega_1 + j\omega_2) = \frac{1}{10^4 - (\omega_1^2 + \omega_2^2) + j10(\omega_1 + \omega_2)}$$

Figure 5 shows the modulus and phase of $H_2(j\omega_1, j\omega_2)$. The most salient features of Figure 5 are the characteristic ridges at 0, 90 and 45 to the two frequency axes, these ridges occurring at the linear resonant frequency, namely 15.9 Hz (100 rad/s). Where two ridges cross there is a peak indicating a resonant condition. Thus if we input a single frequency along one of the 90 ridges we would automatically excite the resonance since $\omega_1, \omega_2 = \omega_r$. However, if we input two frequencies which intersect on the 45° ridges ($\omega_1 + \omega_2 = \omega_r$) then we again excite the resonance condition via an energy transfer mechanism even though neither of these two individual frequencies are numerically equal to the resonance frequency. This represents a 'sum' condition resonance. 'Difference' conditions i.e. ($\omega_1 - \omega_2 = \omega_r$) can also satisfy this energy transfer mechanism. Figure 6 shows a three degree of freedom $H_2(j\omega, j\omega)$ frequency response function. As can be seen, when the order of the complexity of the structure increases, the full H_2 representation is complex and the simplest way of presenting the higher order FRF's is to use the leading diagonal representation.

The magnitude of the $H_2(j\omega, j\omega)$ plane gives an indication of the contribution of the quadratic nonlinear characteristics to the total output. Since $H_2(j\omega, j\omega)$ is a complex function this contribution may, in some cases, reduce the total power output, a form of gain compression or it can increase the total power output via a gain magnification, this being dependent on the phase characteristics of the FRF's. If we were to extend the method to the third order FRF we would be able to visualise the contribution of the cubic characteristics of the nonlinear terms to the response. In this case we would need to plot the ω_1, ω_2 plane for different values of ω_3 such that ω_1 and ω_2 were varied whilst ω_3 was held constant.

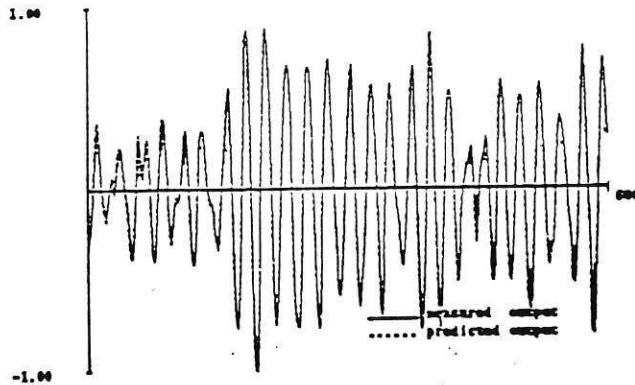
EEC box (Case 2 : Input 0-300 + 150-180)

Data length - 1000 points
 Line search criterion - 0.100e-03
 Stop optimisation criterion - 0.100e-03
 Number of iterations - 9
 Maximum Number iterations - 20

TERMS	ESTIMATES	Stdev
y(t-1) -	0.16022e+01	(0.31342e-02)
y(t-2) -	-.94722e+00	(0.26528e-02)
u(t- 1) -	0.61536e-01	(0.16724e-02)
Constant term -	0.13767e+00	(0.78094e-02)
y(t-1)*y(t- 1) -	-.13810e-01	(0.47595e-03)
y(t-1)*y(t- 1)*y(t- 1) -	-.25251e-02	(0.15085e-03)
e(t- 2) -	0.32458e+00	(0.29373e-01)
e(t- 1) -	-.48221e+00	(0.29209e-01)
e(t- 3) -	0.18078e+00	(0.29136e-01)
e(t- 4) -	0.54324e-01	(0.29130e-01)
e(t- 5) -	0.58697e-01	(0.29140e-01)
e(t- 6) -	0.91727e-01	(0.29234e-01)
e(t- 7) -	0.14711e+00	(0.29250e-01)
e(t- 8) -	0.10123e+00	(0.291583-01)
e(t- 9) -	0.26099e+00	(0.29248e-01)
e(t-10) -	0.19766e+00	(0.29230e-01)

Narmax model is :- y

$$y(t+1) = 1.602y(t) - .947y(t-1) + 0.0615u(t) + 0.937 - 0.0138 y^2(t) - 0.0025y^3(t)$$



Comparison of the measured and predicted o.p's

TABLE 1

5. PRACTICAL RESULTS FROM A TEST STRUCTURE

Tests have been conducted on a clamped-clamped beam rig which was designed to include predominantly quadratic type non-linear behaviour. This was achieved by pre-loading the beam at the central point. The tests concentrated on the first two modes of the structure with the acceleration response of the beam being measured at four points along the beam. Strongly quadratic stiffness behaviour was produced by the pre-load.

Figure 7 shows the measured first and second TFs at a relatively low amplitude of sinewave input. Well-defined second order TF's were obtained whereas the third order TFs were poor (appearing as noise), indicating that for small amplitude deflections, the second order *quadratic* behaviour was more dominant than the third order *cubic* behaviour. In the tests, only TFs up to order three were recorded since it was the objective of the experiment to assess only the linear, quadratic and cubic nature of the beam. Information regarding the higher order terms in the polynomial can be determined by measuring TFs above the third, although the significance of the higher harmonic terms on the output waveform tends to decrease as the order of the harmonic increases.

Visual inspection of the TFs can yield information regarding the system directly.

1. Conventional Modal Testing techniques can be used to analyse and interpret the first order TFs (Fig. 7(a)). The first bending mode of the beam occurs at approximately 85 Hz, and the second at 215 Hz.
2. The higher order TFs exhibit peaks on the magnitude plots at the same frequencies as the first order TF. In addition, modes which behave strongly quadratically have peaks on the second order TFs at half the fundamental resonant frequencies of the mode. From the measurements [Fig. (7b)] it may be concluded that in the first bending mode the beam departs from linearity.
3. The third order TF could not be resolved adequately by the measurement equipment and interpretation of the data is not worthwhile.

It should be noted that if the beam were behaving linearly, no higher order TRF would exist and the second and third order TFs measured would have no recognisable form.

CONCLUSIONS

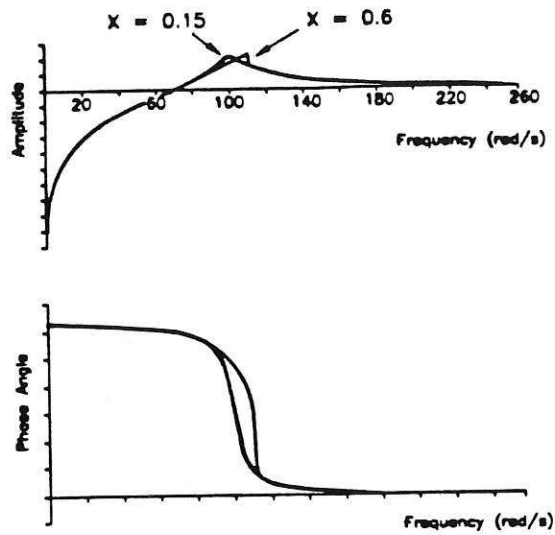
Two approaches to the determination of higher order spectra have been described in this paper, namely the use of stepped sine tests to obtain the higher order transfer functions and the Narmax method to extract the higher order frequency response functions. The stepped sine procedure is a conventional frequency domain method whereas the Narmax approach requires an indirect step to obtain a difference model from discrete time data from which the FRF's can be computed. If reliable higher order FRF's can be measured/obtained then one gains a powerful insight into a class of nonlinearities and they have the potential to accurately detect frequency ranges e.g. modes where nonlinearity is significant. They also offer an immediate visual inspection of nonlinearity and can be used to investigate the possibility of energy transfer from one frequency (mode) to another. However, higher order spectra have had little application in the field of structural dynamics and until they have been evaluated in practise it would be premature to place an emphasis on their usefulness.

ACKNOWLEDGEMENTS

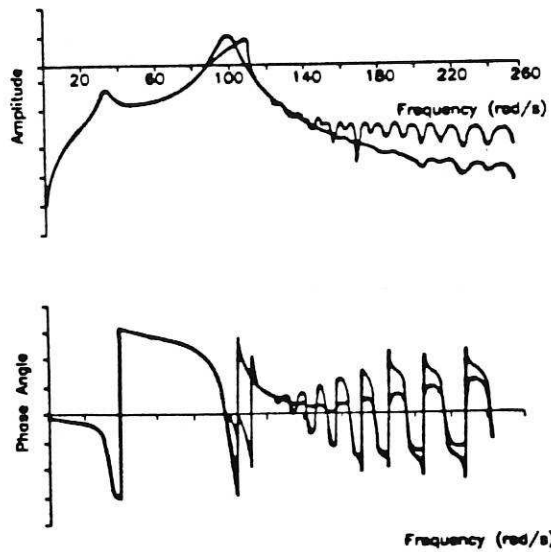
The authors would like to acknowledge the help of D. Storer, Research Assistant in the Dynamics Research Group at Manchester University who provided many of the results for this paper.

REFERENCES

1. K.I. Kim and E.J. Powers "A digital method of modelling quadratically nonlinear systems with a general random input", IEEE Trans.Acous.,Speech, Signal Proc. Vol. ASSP-36 pp1758-1769, 1988.
2. S.W. Nam, S.B. Kim and E.J. Powers "Utilisation of digital polyspectral analysis to estimate transfer functions of cubically nonlinear systems with nonGaussian inputs", IEEE Trans.Acoust.Speech, Signal Proc., Paper E6.1, pp 2306-2309, 1989.
3. S.J. Gifford and G.R. Tomlinson, "Recent advances in the application of functional series to nonlinear structures", Jnl. Sound and Vibration, 135(2), 289-317, 1989.
4. S.A. Billings and K.M. Tsang, "Part I : Parametric nonlinear spectral analysis", Mech. Systems and Signal Proc., 3, 319-339, 1989.
5. S.A. Billings and W.S.F. Voon, "Structure detection and model validity tests in the identification of nonlinear systems", Proc. IEEE, 130, Pt.D, No.4, 193-199, 1983.
6. M. Korenburg, S.A. Billings et al, "Orthogonal parameter estimation algorithm for nonlinear stochastic systems", Int. Jnl. Control, 48, No.1, 193-210, 1988.
7. E. Bedrossian, and S.O. Rice, "The output properties of Volterra Systems", IEEE, 59, 1688-1707, 1971.



(a)

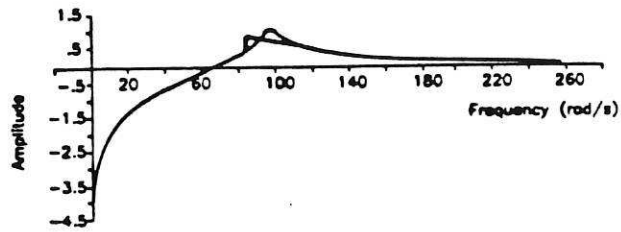


(b)

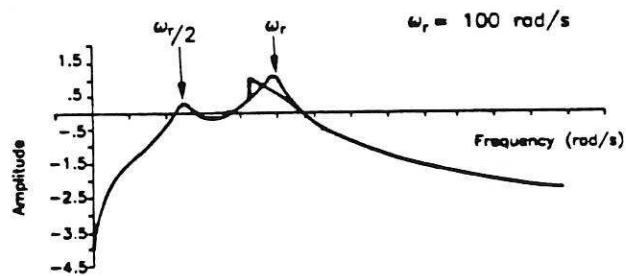
Figure 1 (a) 1st Order TF } Simulated from
 (b) 3rd Order TF } the Equation

$$\ddot{y}(t) + 10\dot{y}(t) + 10^4 y(t) + 10^{10} y(t)^3 = X \cos \omega t$$

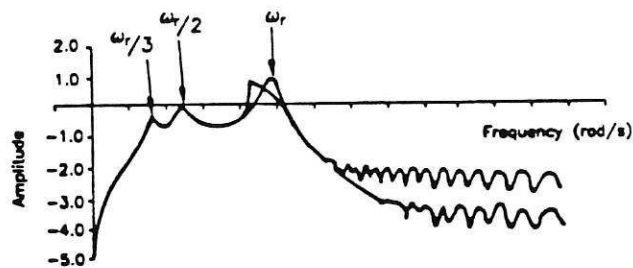
(a) $X = 0.15$; (b) $X = 0.6$



(a)



(b)



(c)

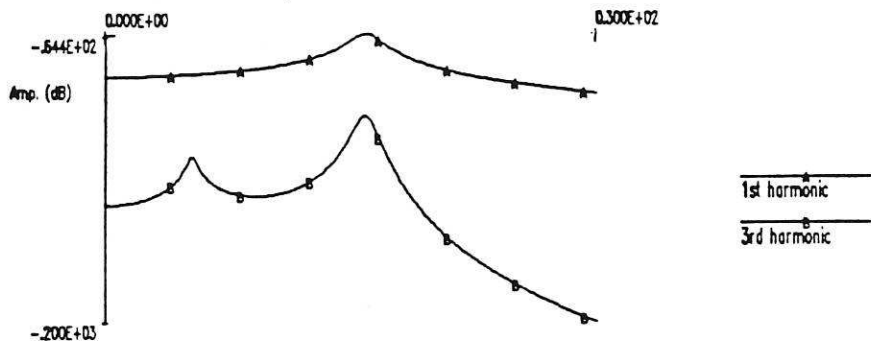
Figure 2: (a) 1st Order TF

(b) 2nd Order TF

(c) 3rd Order TF

$$\ddot{y} + 10\dot{y} + 10^4 y + 10^7 y^2 = X \cos \omega t$$

$$X = 0.15; 0.6$$



LEADING DIAGONALS OF H_1, H_3

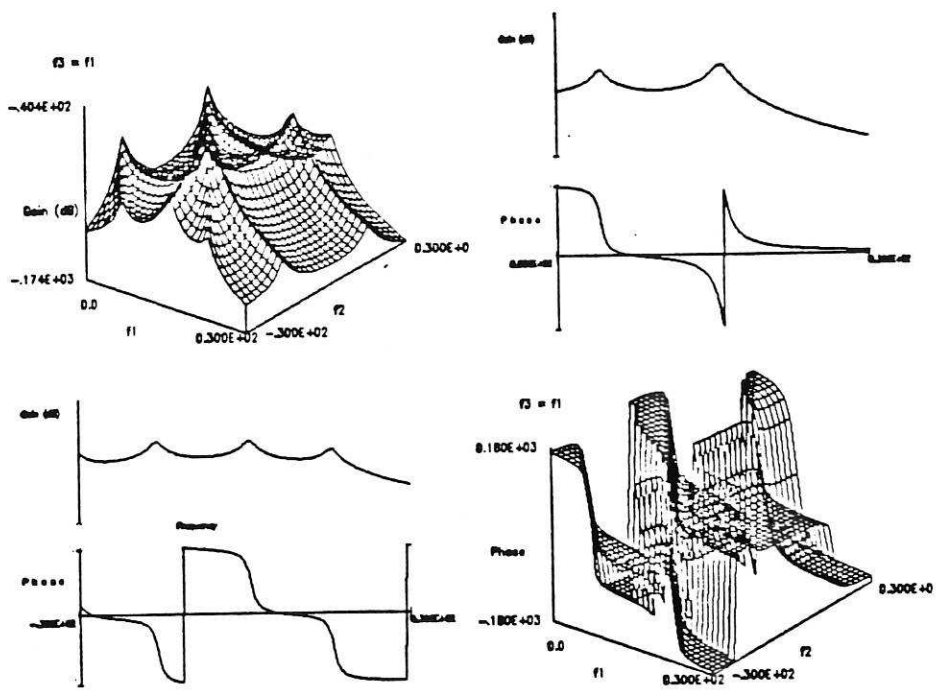


FIGURE 3(a) : $H_3(j\omega_1, j\omega_2, j\omega_3)$ FROM THE MODEL $y + 10y + 10^4 + 10^{10}y^3 = u(t)$

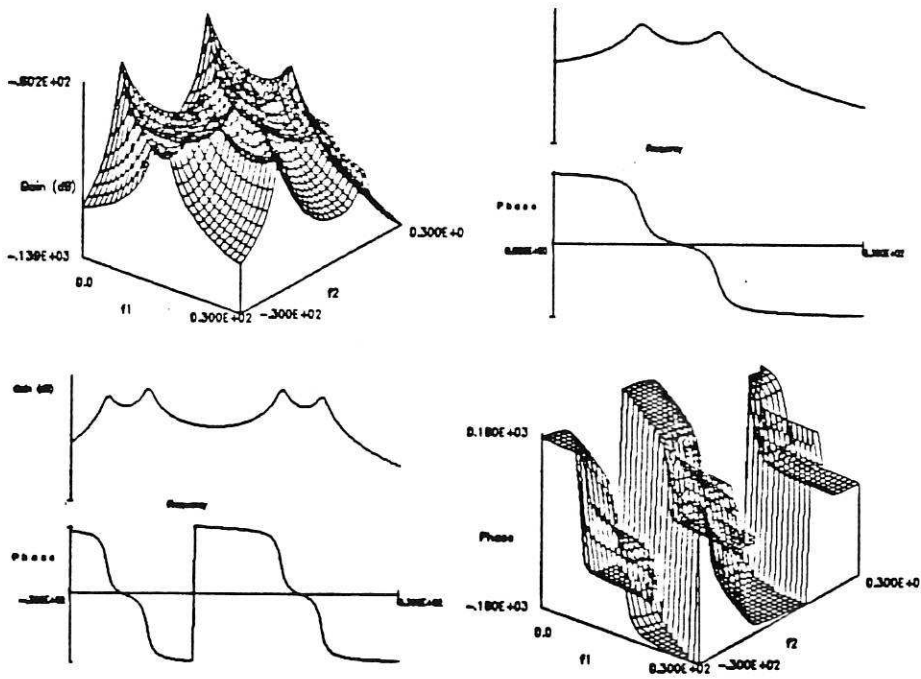
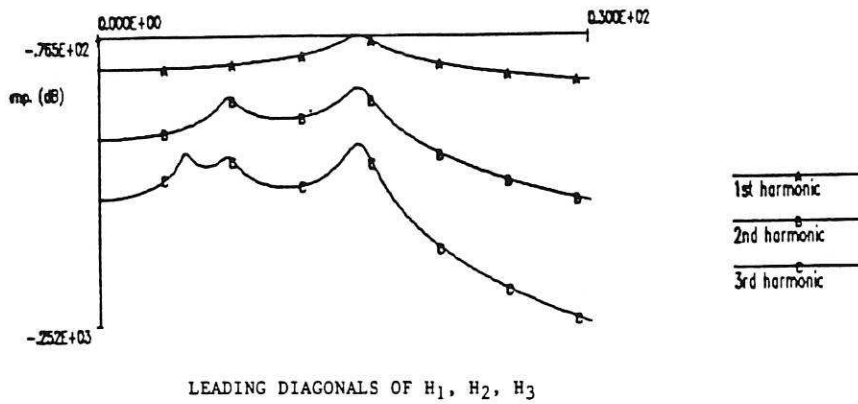


FIGURE 4 : 3D PLOT OF H_2 FROM THE MODEL $\dot{y} + 10y + 10^4 + 10^7y^2 = u(t)$

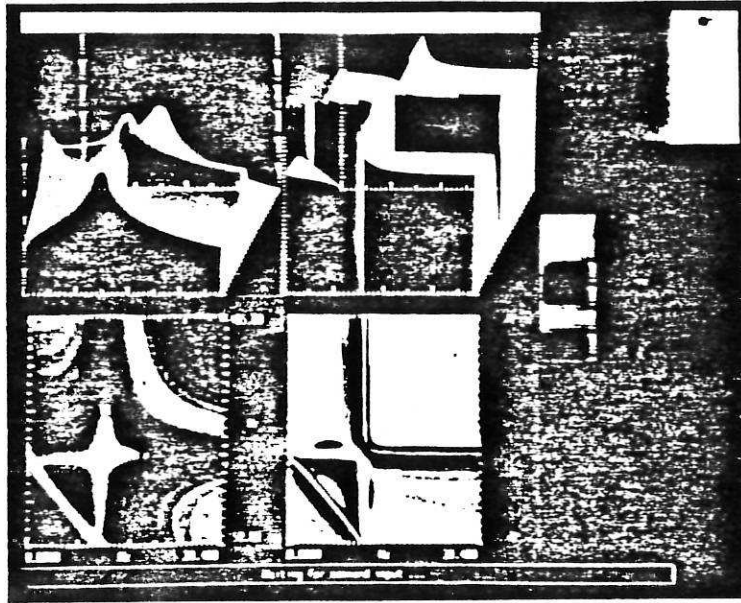


FIGURE 5 : MODULUS AND PHASE OF A SECOND ORDER FRF i.e. $H_2(j\omega, j\omega)$

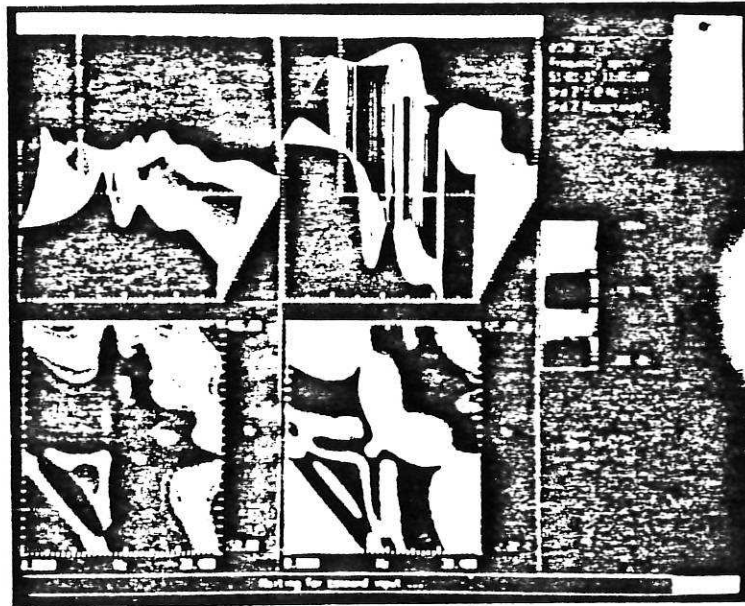
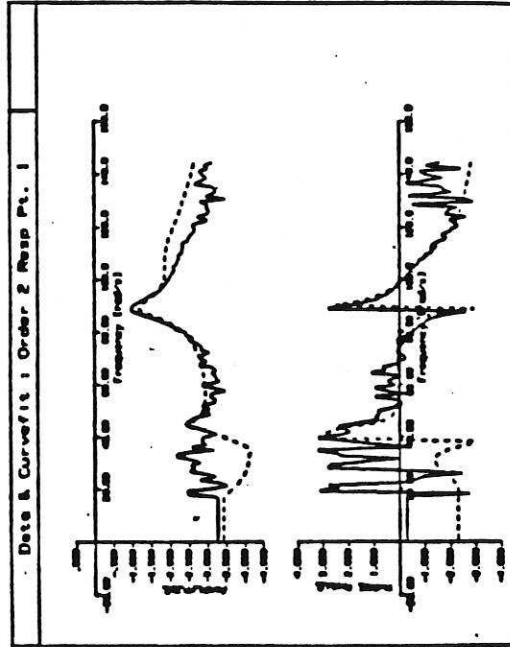
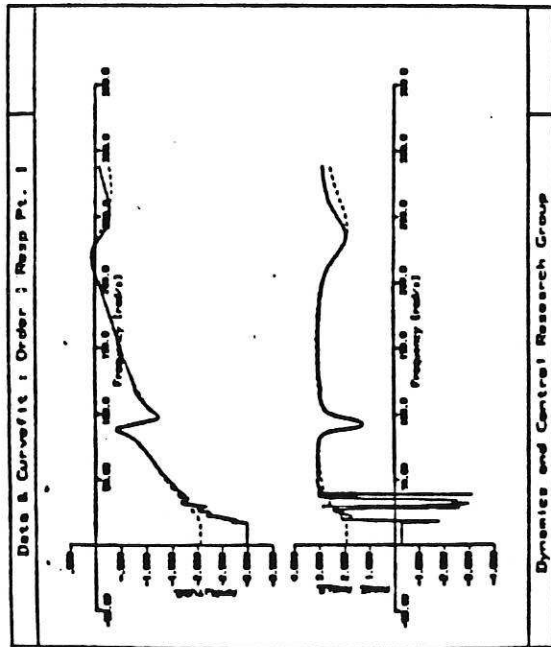
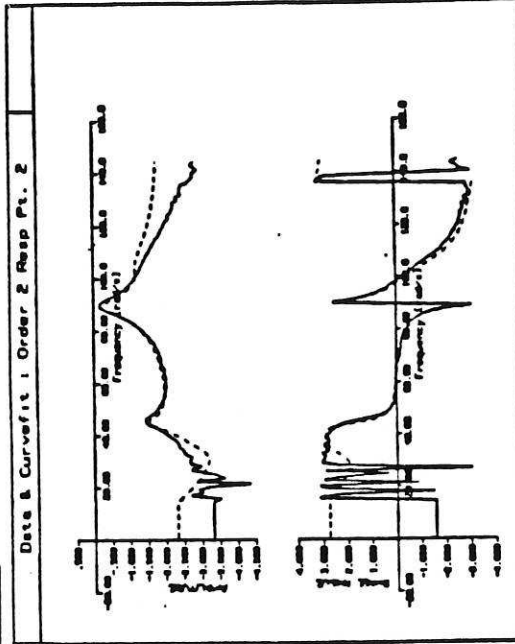
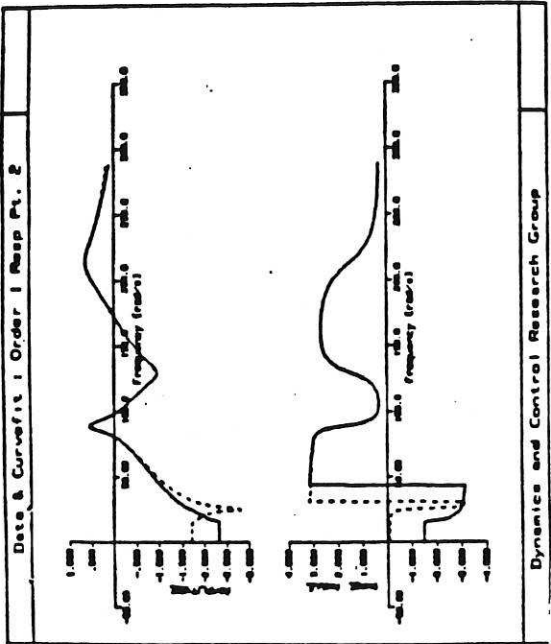


FIGURE 6 : $H_2(j\omega, j\omega)$ FOR A THREE DEGREE OF FREEDOM SYSTEM



DATA ----- CURVE FIT

FIGURE 7(a) : EXPERIMENTAL 1st and 2nd ORDER TRANSFER FUNCTIONS
SPATIAL POINT No. 1



DATA ----- CURVE FIT

FIGURE 7(b) : EXPERIMENTAL 1st and 2nd ORDER TRANSFER FUNCTIONS
SPATIAL POINT No. 2

